

## Rutherford Backscattering

Named for Ernest Rutherford who worked on alpha particle scattering

- Rutherford proposed the nuclear atom, based on experiments by Hans Geiger and Ernest Marsden in 1911  
(Geiger and Marsden worked in Rutherford's lab)

Amazing finding was that the scattering amplitude to angles  $> 90^\circ$  was about  $10^{-4}$  but had been predicted  $< 10^{-3500}$  based on the uniformly distributed charge model (i.e. Thomson model)



Ernest Rutherford (1871–1937, England). Founder of nuclear physics, he is known for his pioneering work on alpha-particle scattering and radioactive decays. His inspiring leadership influenced a generation of British nuclear and atomic scientists.

- Kenneth Krane,  
"Modern Physics", 1st Ed.  
p. 157

In Rutherford's model, the charge and mass are concentrated in a tiny "nucleus"

The incident charged particle interacts with the ~~charged nucleus~~ charged nucleus via

$$F = \frac{(ze)(Ze)}{4\pi\epsilon_0 r^2}$$

The paths taken by such particles are hyperbolic trajectories.

$$\frac{1}{r} = \frac{1}{b} \sin \phi + \frac{zZe^2}{8\pi\epsilon_0 b^2 K} (\cos \phi - 1)$$

or

$$b = \frac{zZe^2}{8\pi\epsilon_0 K} \cot \frac{1}{2}\theta = \frac{zZ}{2K} \frac{e^2}{4\pi\epsilon_0} \cot \frac{1}{2}\theta$$

using  ~~$\phi = \pi - \theta$~~   $\phi = \pi - \theta$ ,  $r \rightarrow \infty$   
 smaller  $b$  (impact parameter)  
 leads to larger  $\theta$  (scattering angle)

The fraction scattered to angles  $> \theta$  will be

$$f_{>\theta} = f_{<b} = (nt)\pi b^2$$

↑  
 number of nuclei  
 per unit area

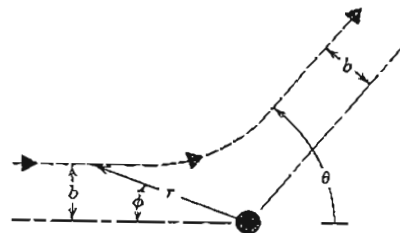


FIGURE 6.8 The hyperbolic trajectory of a scattered particle.

Krane, p. 155

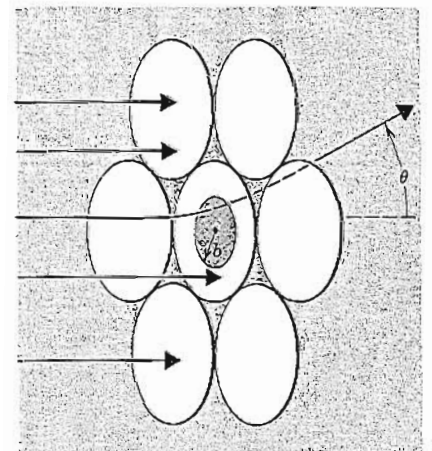


FIGURE 6.9 Scattering geometry for many atoms. For impact parameter  $b$ , the scattering angle is  $\theta$ . If the particle enters the atom within the disc of area  $\pi b^2$ , its scattering angle will be larger than  $\theta$ .

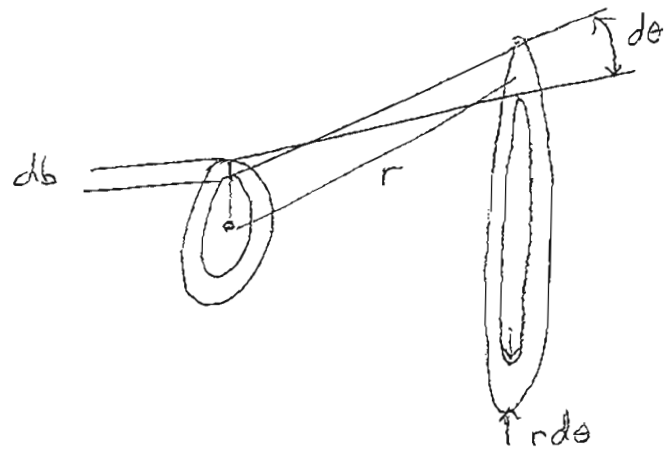
- Krane, p. 155

Krane p. 155

From here we calculate

$$df = (nt) 2\pi b db$$

$$db = \frac{zZ}{2K} \frac{e^2}{4\pi\epsilon_0} (-\csc^2 \frac{\theta}{2}) (\frac{1}{2} d\theta)$$



using  $dA = (2\pi r \sin\theta) r d\theta$

$$\Rightarrow N(\theta) \equiv \frac{|df|}{dA} = \frac{(nt)}{4r^2} \left(\frac{zZ}{2K}\right)^2 \left(\frac{e^2}{4\pi\epsilon_0}\right)^2 \frac{1}{\sin^4(\frac{\theta}{2})}$$

Rutherford Scattering Formula

This is similar to the Rutherford Scattering "Cross Section"

$$\frac{dS}{d\Omega} = -\frac{b}{\sin\theta} \frac{db}{d\theta} = \left(\frac{Z_1 Z_2}{2E_1}\right)^2 \left(\frac{e^2}{4\pi\epsilon_0}\right)^2 \frac{1}{\sin^4(\theta/2)}$$

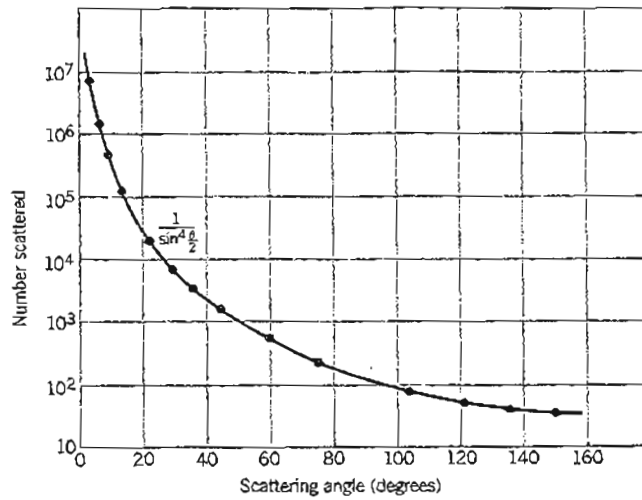


FIGURE 6.15 The dependence of scattering rate on the scattering angle  $\theta$ , using a gold foil. The  $\sin^{-4}(\theta/2)$  dependence is exactly as predicted by the Rutherford formula.

Krane, p. 159

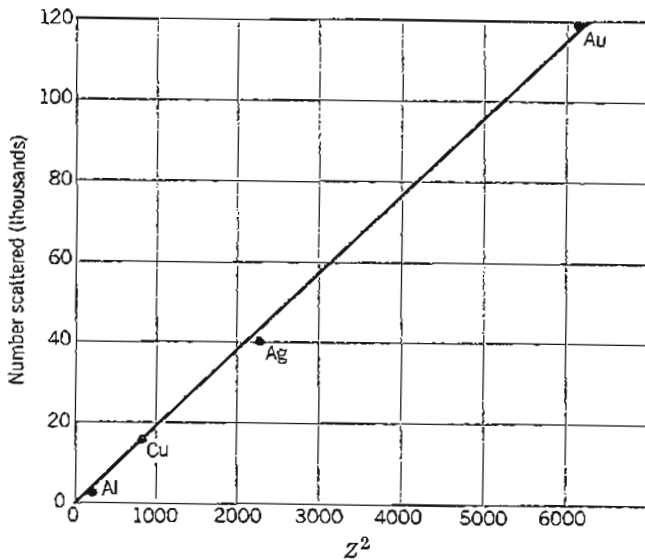


FIGURE 6.13 The dependence of scattering rate on the nuclear charge  $Z$  for foils of different materials. The data are plotted against  $Z^2$ .

Krane, p. 158

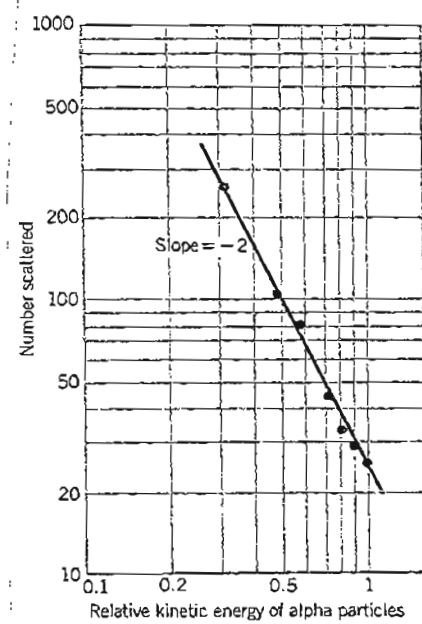
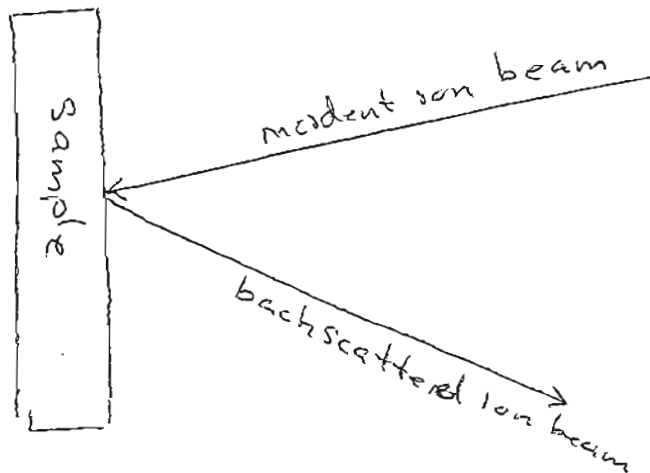


FIGURE 6.14 The dependence of scattering rate on the kinetic energy of the incident alpha particles for scattering by a single foil. Note the log-log scale; the slope of  $-2$  shows that  $\log N \propto -2 \log K$ , or  $N \propto K^{-2}$ , as expected from the Rutherford formula.

Krane, p. 158

In the technique of Rutherford Backscattering as we know it today, an incident beam of ions impinges on the sample of interest, and the backscattered intensity is measured.

The incident angle and angle of collection are also varied.



Some of the ions penetrate into the sample and remain there.

At particular angles where the incident beam is parallel to ~~the~~ crystal directions of high symmetry, an effect called "channeling" can occur.

As long as the energy of the incident ion is large, there will be little effect of the electron "cloud". The scattering is dominated by the nuclei,

Lüth explains at lower energies the scattering potential is modified due to screening.

In any case, ~~there is~~ an effect called shadowing will occur.

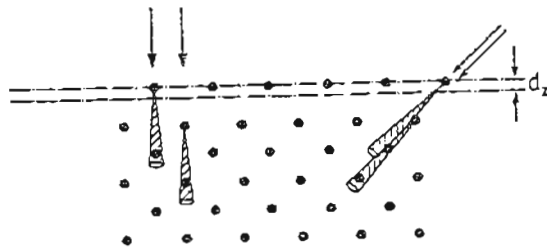


Fig. 4.33. Sectional view of a surface with relaxation  $d_z$  of the topmost atomic layer showing high-energy ion scattering shadow or blocking cones for incidence along two bulk channelling directions [4.27]

Lüth, p. 202

Incident ions which do not encounter closely a surface nucleus will be channelled.

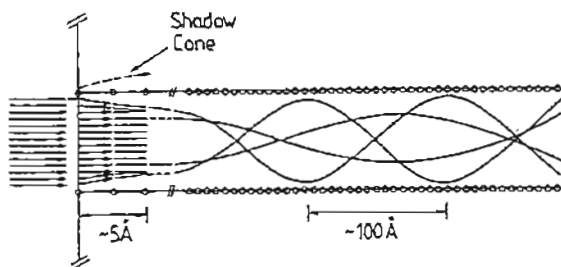


Fig. 4.34. Schematic representation of particle trajectories undergoing scattering at the surface and channeling within the crystal. The depth scale is compressed relative to the width of the channel in order to display the shape of the trajectories [4.25]

Lüth, p. 203

These effects can be utilized to study the structure and composition of thin films, even giving information about the top-most atomic layers.

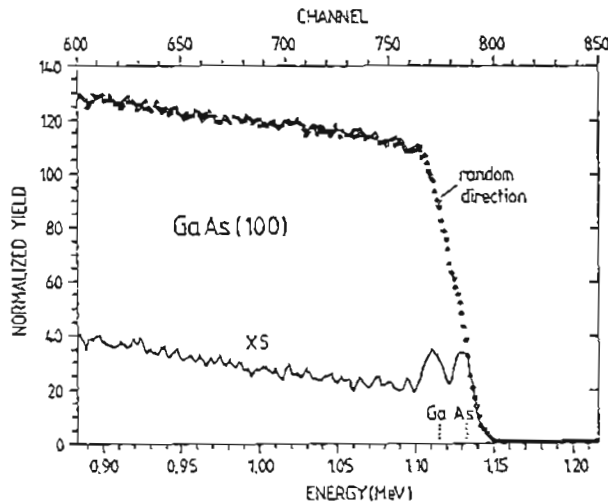


Fig. 4.35. Ion backscattering yield spectra of 1.4-MeV  $\text{He}^+$  from a GaAs(100) surface along a "random" non-channeling direction and along the surface normal (100), amplified by a factor of 5 [4.29]

Lüth, p. 204

This graph shows the extreme sensitivity of the backscattering to the incidence angle.

For the aligned case, the backscattering is strongly reduced, and the surface top atomic layer causes two peaks.

The energy separation can be ascribed to a small recoil effect. For example,

$$m_{\text{As}} > m_{\text{Ga}}$$

so the scattering off As loses less energy to recoil. The backscattered particle has greater energy.

A variety of different film types and surface configurations can be successfully studied using RBS

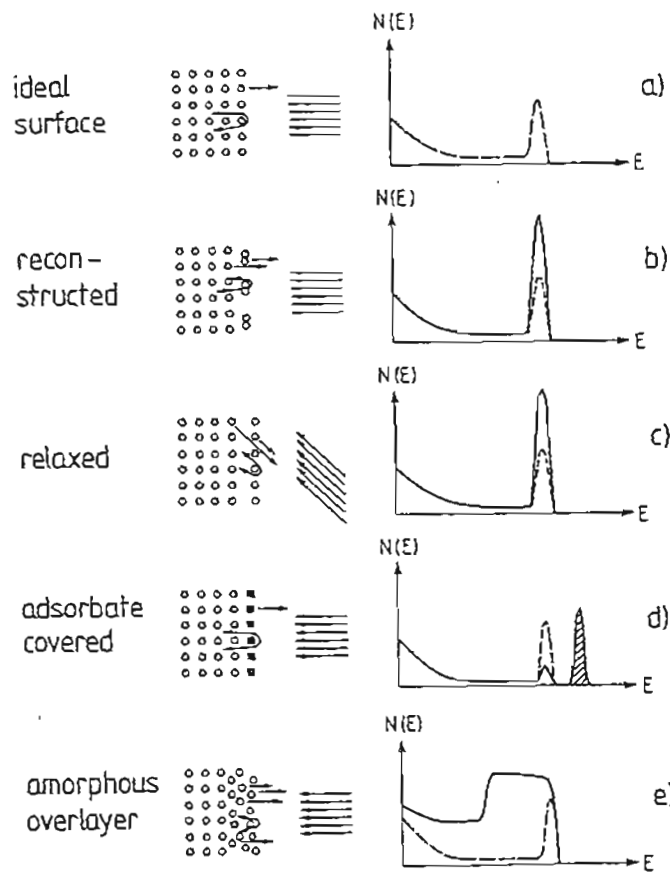


Fig. 4.36a-e. Qualitative overview of some applications of ion backscattering and the corresponding spectra  $N(E)$ : (a) Scattering from an ideal clean crystal surface under channeling conditions. The backscattering spectrum (dashed curve) consists of a *surface peak* due to scattering on the topmost atomic layer and a low intensity plateau at lower kinetic energies which arises from scattering events deep in the bulk. (b) Scattering on a reconstructed surface causes a considerable increase of the surface peak (up to double intensity) in comparison with the ideal surface spectrum (dashed curve). The second atomic plane contributes to the scattering events due to incomplete shadowing. (c) For a relaxed surface, non-normal incidence under channeling conditions causes a similar intensity increase of the surface peak due to incomplete shadowing (dashed curve: spectrum of unrelaxed ideal surface). (d) Scattering on an ideal surface covered with an adsorbate overlayer under channeling conditions. The adsorbate layer gives rise to a second surface peak (shaded) due to scattering on atoms with different mass. Due to shadowing, the original surface peak (dashed curve) is reduced in intensity. (e) Scattering on a crystal covered with an amorphous overlayer gives rise to a broad plateau instead of a sharp surface peak. Many atoms out of registry contribute to the scattering in deeper layers. For comparison, the dashed line shows the spectrum for scattering on an ideal crystal surface [4.25]

A depth scale can also be related to the energy scale using a mathematical model,

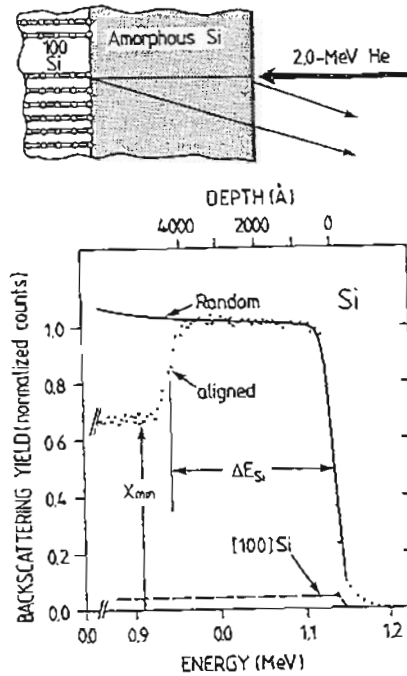


Fig. 4.37. Backscattering channeling spectrum (ion yield versus kinetic energy) of a 4000-Å thick amorphous Si-layer on top of a Si(100) surface. The spectrum was obtained under channeling conditions with 2-MeV  $^4\text{He}$  ions (inset). Using a mathematical model for the Rutherford backscattering processes, the energy scale is converted into a depth scale (upper abscissa). For comparison, the spectra of the Si surface before amorphization are also given, for channeling conditions by the dashed line, and for "random" conditions by the full line [4.28]

Another intriguing use of RBS is to determine the site of impurities in a crystal. In particular, you can tell whether an impurity is on a lattice site, or whether it is at an interstitial position.

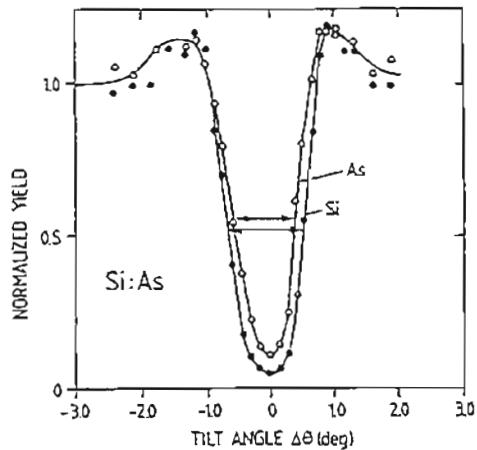


Fig. 4.38. Angular dependence of the backscattering yield around the channeling direction (tilt angle  $\Delta\theta = 0$ ) for 1.8 MeV He ions on a Si-film, which is doped with  $1.5 \cdot 10^{21}$  As atoms/cm<sup>3</sup>. The angular dependence of the Si and of the As backscattering peak are compared [4.30]

Lüth, p. 207

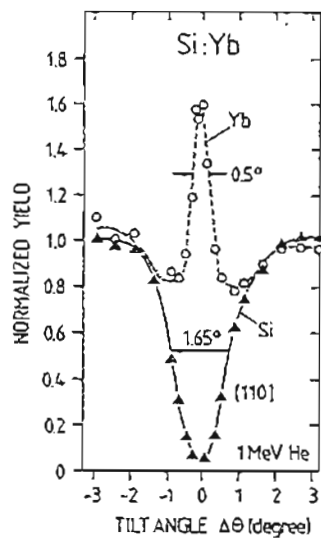


Fig. 4.39. Angular dependence of the backscattering yield (normalized) around the [110] channeling direction (tilt angle  $\Delta\theta = 0$ ) for 1 MeV He ions on a Si film, into which  $5 \cdot 10^{14}$  Yb atoms/cm<sup>2</sup> are implanted (60 keV, 450°C). The Si signal ( $\blacktriangle$ ) is compared with the Yb signal (o) [4.31]

Lüth, p. 207